paper kimia valensi

by Ferli Irwansyah

Submission date: 22-Jan-2025 08:41PM (UTC+0700)
Submission ID: 2569021393
File name: 41699-130399-1-PB.pdf (682.65K)
Word count: 4949
Character count: 25967

JURNAL KIMIA VALENSI
p-ISSN: 2460-6065; e-ISSN: 2548-3013
Journal homepage: https://journal.uinjkt.ac.id/index.php/valensi
Research Article

Characterization and Application of Hydroxyapatite From Chicken Egg Shell with Green Template as a Potential Drug Delivery System

Ferli Septi Irwansyah[1*], Abshar Fathur Rochman Nurizal[2], Eko Prabowo Hadisantoso[2], Shariffuddin Bin Md Zain[3]

[1]*Department of Chemistry Education, UIN Sunan Gunung Djati Bandung, 40292, Indonesia*
[2]*Department of Chemistry, UIN Sunan Gunung Djati Bandung, 40614, Indonesia*
[3]*Department of Chemistry, University of Malaya, 50603, Malaysia*

[*]*Email: ferli@uinsgd.ac.id*

Article Info
Received: Oct 6, 2024
Revised: Oct 7, 2024
Accepted: Nov 28, 2024
Online: Dec 16, 2024

Citation:
Irwansyah, F. S., Nurizal, A. F. R., Hadisantoso, E. P., Zain, S. B, M. (2024). Characterisation and Application of Hydroxyapatite From Chicken Egg Shell with Green Template as a Potential Drug Delivery System. *Jurnal Kimia Valensi*, 10(2), 260-268

Doi: 10.15408/jkv.v10i2.41699

Abstract

Hydroxyapatite (HAp) is a calcium phosphate biomaterial widely studied in the medical field because of its good biocompatibility properties. This study aims to identify the effect of increasing variations in banana peel template concentration on the characteristics of hydroxyapatite so that it has the potential as a drug delivery system. This study includes the characterization and application of the potential of the hydroxyapatite drug delivery system with the addition of variations in the concentration of green template. Then, hydroxyapatite was characterized using X-ray diffraction (XRD) and a surface area analyzer (SAA). This study's results indicate that adding a banana peel template affects the characteristics of hydroxyapatite. The higher the template concentration, the smaller the crystallite size, pore size, pore volume, and surface area, but the degree of crystallinity is greater. The results showed that the characterization of hydroxyapatite K15% with a crystal size of 34.73, a degree of crystallinity of 89%, a pore size of 7.2178 nm, a surface area of 30.111 m^2/g, and a pore volume of 0.1145 cc/g. The results of the study of the potential of the drug delivery system obtained a loading efficiency value of 67% for ibuprofen. However, the ibuprofen release process results at time intervals tend to be unstable.

Keywords: Egg shell, hydroxyapatite, banana peel, drug delivery system

1. INTRODUCTION

Hydroxyapatite (HAp) is a calcium phosphate biomaterial widely studied in the medical field due to its high biocompatibility and similarity to the structure of human bones [1]. However, hydroxyapatite used in Indonesia still comes from other countries, so it is necessary to develop research on hydroxyapatite synthesis. Biomaterials are materials or medical devices that can be synthetic, biological, or a mixture of both to regenerate or replace body parts or tissues or help, add, or restore body functions. Applications are extensive in the medical field, such as scaffolds [2] and drug delivery [3].

HAp can be synthesized using natural precursors such as calcium and phosphate. Usually, HAp synthesis uses precursors in the form of phosphoric acid (H_3PO_4) and calcium hydroxide ($Ca(OH)_2$). Currently, many researchers are studying chicken eggshells as an alternative to HAp synthesis because chicken eggshells contain high calcium carbonate ($CaCO_3$) elements, known to contain 91.60% [4]. HAp from natural sources contains ions, such as Na^+, Zn^{2+}, Mg^{2+}, K^+, Si^{2+}, Ba^{2+}, F^- and CO_3^{2-} [5].

The HAp synthesis process greatly determines hydroxyapatite particles' morphology, crystallography, and phase purity in crystal size, surface area, porosity, and adsorption capacity. It is the fact that materials with smaller sizes are more reactive and show increased physicochemical properties due to the larger open surface area, which ultimately determines the final properties of the material for use in biomedical applications [6]. To ensure that the synthesized HAp is on a nanoscale or to control its agglomeration and morphology, it is necessary to pay attention to the synthesis method used [7].

Plant extracts mediate the most widely used synthesis method for nanoparticles. Plant extracts are alternative chemicals that are widely used to anticipate agglomeration. HAp mediated by plant extracts offers an environmentally friendly method. In addition to its environmentally friendly nature, natural sources act as reducing agents and stabilizers of the product and control the shape and size of the particles. Banana peel extract is known to contain phytochemicals with anti-inflammatory and antioxidant properties. Banana peel is considered a good source of nutrition with bioactive phenolics, antioxidants, and potassium [8].

Banana peel contains various compounds such as reducing sugars and antioxidant compounds (phenolic compounds, alkaloids, tannins, and flavonoids) more than other parts [9 10 11]. It is known that the flower, fruit skin, and banana stems contain phenolic and flavonoid compounds of 1.69% and 0.33%, respectively [12]; 5.65% and 2.25% [13]; also 2.91% and 0.80% [14] per 100 grams of dry sample weight.

Banana peel is known to regulate the shape and size of crystals and overcome agglomeration barriers during HAp production compared to other parts. It is in accordance with what Alfi did in 2023 that adding banana plant part templates (flowers, fruit skin, and stems) can reduce the crystal size and increase the degree of crystallinity from XRD characterization. In FTIR characterization, no OH-bonds were detected, indicating the presence of water in the flowers and fruit skin. In the PSA characterization results, increasing the concentration of banana peel can reduce particle size by up to 45%[15].

Banana peel contains pectin, which plays a role in forming HAP crystals. It is known that the pectin content in banana peel varies greatly, around 1.92–3.2[6]% of its dry weight. Pectin is also identified as being rich in carboxyl and [6]ydroxyl groups, which act as stimulants for binding calcium ions (Ca^{2+}) from solution to carboxylate ions, which causes the nucleation process of hydroxyapatite crystal growth [16]. The content has biocompatible, biodegradable, antimicrobial, anticoagulant, and anti-inflammatory properties. So, this banana peel has shown potential in biomedical applications in drug delivery systems.

2. RESEARCH METHODS

Materials and Instruments

The materials used in this study were $(NH_4)_2HPO_4$ (Merck® p.a.), NH_4OH (25% Merck® p.a.), acetone (technical), 96-w[18] plate, cisplatin, dimethyl sulfoxide (DMSO), PrestoBlueTM Cell Viability Reagent, Roswell Park Memorial Institute Medium (RPMI), Fetal Bovine Serum (FBS), Antibiotics (Sigma Aldrich P4333), CV-1 cells, Trypsin-EDTA, Trypan Blue, Ibuprofen, SBF media, deionized water, filter paper, chicken egg shells, and banana fruit peels.

The instruments used include X-ray Diffraction (XRD), NOVAe Surface Area Analyzer (SAA), Quantachrome Novatouch Lx4 brand with Brunauer-Emmett-Teller (BET) method, CO_2 Incubator (Thermo Scientific Series 8000DH), Microscope (Thermo Scientific EVOS XL Core), Multimode Reader (Tecan Infinite M200 PRO), centrifugation, incubator shaker, and UV-Vis spectrophotometer.

Calcination of Chicken Egg Shells

One hundred grams of chicken eggshell waste was washed with tap water several times. Then, it was rinsed using Aqua DM. Next, it was ground with a mortar and pestle and sieved with a 120 mesh sieve. The sieving results were then calcined at 1000 °C for 5 hours.

Extraction of Template from Banana Peel

[6]ve hundred grams of banana peel were cleaned, washed with distilled water, rinsed with acetone, and then cut into smal[24]ieces. The cut part was dried in the sun for 4 hours, then dried again using an oven at 60 °C for 24 hours, and then heated in 250 mL of water for 10 minutes. Then, the banana peel was filtered, and the filtrate was used as a green template for the next process.

Synthesis of Hydroxyapatite with Green Template

2.8625 g of calcium oxide (CaO) from the calcination results and 3.9431 g [33]diammonium hydrogen phosphate ($(NH_4)_2HPO_4$) were put into a 200 mL autoclave. Then, 50 mL of deionized water and 5 mL of template from each variation were added and stirred until evenly distributed. Next, ammonium hydroxide solution (NH_4OH [5]vas added drop by drop while stirring to maintain a pH of 10. After that, th[35] mixture was heated in an autoclave in an oven at a temperature of 230 °C for 48 hours. Nex[4] the mixture was filtered, and the residue was washed with deionized water until pH 7. [29]en, the residue from the washing was dried at 110 °C for 24 hours. After that, the residue was ground to get a more uniform size. The result of this refinement is HAp material, which can then be characterized

Hydroxyapatite Characterization

An XRD (X-ray diffraction) instrument uses X-ray tube rays in the form of CuKα (1.54060 Å) for testing crystal size analysis, degree of crystallinity, and crystal structure. Furthermore, the SAA (surface area analyzer) brand Quantachrome Novatouch Lx4 is used by removing adsorbed gas (degassing), and then nitrogen gas is used for the analysis process. Testing

the analysis of pore size, pore volume, and surface area using the BET method (Brunauer-Emmett-Teller).

Hydroxyapatite Application

The application of synthesized hydroxyapatite as a potential drug delivery system was carried out on the most optimal characterization results, HAp K15%, because of the better crystal size and surface area. Toxicity testing was carried out on HAp K15% on normal cells as a parameter for biomedical applications. Furthermore, drug loading and drug release capabilities were tested on ibuprofen as a requirement for the drug delivery system.

3. RESULTS AND DISCUSSION

Preparation of Precursors

In the calcination process, $CaCO_3$ begins to break down or decompose into CaO at a temperature of 750 °C, then wholly breaks down at 1000 °C . The reactions that occur are:

$$CaCO_{3(s)} \xrightarrow[1000°C]{} CaO_{(s)} + CO_{2(g)} \quad (1)$$

In the calcination process of $CaCO_3$ into CaO, there is a weight reduction because CO_2 gas is another product of the decomposition process. This process is accompanied by a change in color in the CaO material to become whiter with finer grains; this indicates that the degradation process of organic material is no longer occurring. $CaCO_3$ decomposes due to combustion power into CaO by 56.40%. The CaO produced is then used as a calcium precursor in the reaction of hydroxyapatite formation with $(NH_4)_2HPO_4$ as a phosphate precursor and banana peel as a green template precursor after the reaction. Banana peel extract is used because it can help control morphology and reduce crystal size compared to flowers and stems [15].

$$10CaO_{(s)} + 6(NH_4)_2HPO_{4(s)} + 4H_2O_{(aq)} \rightarrow Ca_{10}(PO_4)_6(OH)_{2(s)} + 12NH_4OH_{(aq)} \quad (2)$$

Figure 1. Egg shell A) before and B) after the calcination process

Characterization of HAp using XRD

The HAp XRD data were compared with the HAp standard database. The analysis results can be seen in **Figure 2** and **Table 1**. The crystals crystallographic characteristics can be determined from the X-ray diffraction pattern. Typical HAp peaks in the diffractogram of the synthesized sample appear at 2θ = 25°, 31°, and 32°. However, in addition to these peaks, other peaks indicate the presence of impurity phases at 2θ = 17.9°. The ICSD database compared these peaks: 01-089-6440. In addition, it is known that the crystal structure of the synthesized HAp obtained is hexagonal with a space group of P63/m. The degree of crystallinity is determined by comparing the crystal area fraction with the sum of the crystal area fraction and the amorphous area that can be calculated from the XRD data in Equation (3). Furthermore, the crystallite size can be determined using the Debye-Scherrer equation, Equation (4) below:

$$Xc = 100 \times \frac{(I_{300} - V_{112/300})}{I_{300}} \quad (3)$$

Where I_{300} is the intensity of the diffraction peak at (300), $V_{112/300}$ is the intensity (112) and (300). The purity of HAp K5% is 70.34%, HAp K10% is 74.06%, and HAp K15% is 89.77%. It proves that the low solid/liquid ratio affects the crystallinity of the HAp obtained, although not much.

$$D = \frac{K\lambda}{\beta \cos\theta} \quad (4)$$

This equation requires the FWHM value; this value can be found using the Highscore software or can also be found using the Gaussian method in the Origin software. Next, D is the crystallite size, β is the Full Width at Half Maximum (FWHM) in radians, k is the Scherrer constant (0.9), λ is the X-ray wavelength of Cu Kα radiation, which is 1.5406 A, and θ is the Bragg angle.

After obtaining the shape and group space of the HAp sample, an analysis is carried out by comparing the lattice parameters of each variation of the NHA synthesis results with the lattice parameters of the standard compound to show that the synthesis results are truly HAp. Shown in the **Table 1**.

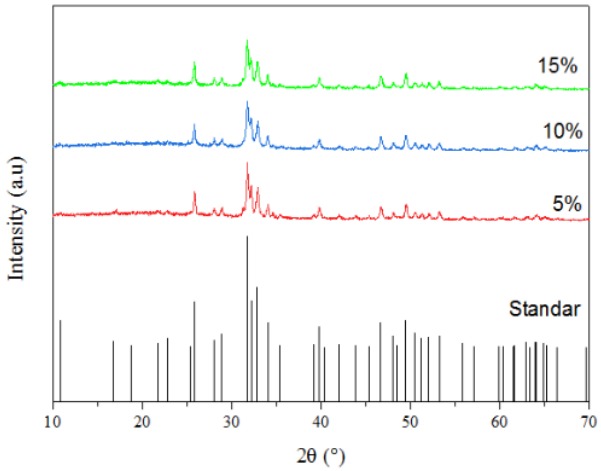

Figure 2. XRD diffraction patterns for each variation of HAp synthesis results

Table 1. Lattice Parameters of NHA Synthesis Results from Each Variation

Sample	Lattice Parameters			
	a=b (Å)	c (Å)	α = β (°)	γ(°)
HAp Standart	9,4240	6,8860	90	120
HAp K5%	9,3869	6,8882	90	120
HAp K10%	9,4429	6,8882	90	120
HAp K15%	9,4459	6,8841	90	120

Several sources affect the purity of the XRD test results. Some of the causes are the presence of contamination of raw materials used in the synthesis, which can cause additional diffraction peaks that are not indexed in the XRD pattern; improper synthesis processes such as temperature or time so that the synthesis does not run optimally, and the use of doping can also cause impurities; if the dopant is not evenly distributed, it will produce additional diffraction peaks or change the position of the existing diffraction peaks[17].

Table 2 shows that the higher the template concentration, the smaller the crystal size and the higher the degree of crystallinity. The role of banana peel templates greatly affects the HAp synthesis process. In addition to the high phytochemical content, banana peels contain pectin in varying amounts. The pectin content in banana peels is around 1.92%–3.25% of the dry weight [18]. This increase occurs because the template's content is cross-linked with Ca^{2+} to form a Ca-template complex through electrostatic and ionic interactions between Ca^{2+} and the carboxyl and hydroxyl groups located in phenolic and flavonoid compounds on the template. This complex then reacts with PO_4^{3-} to form HAp crystallites. This mechanism is in accordance with the **Figure 3**.

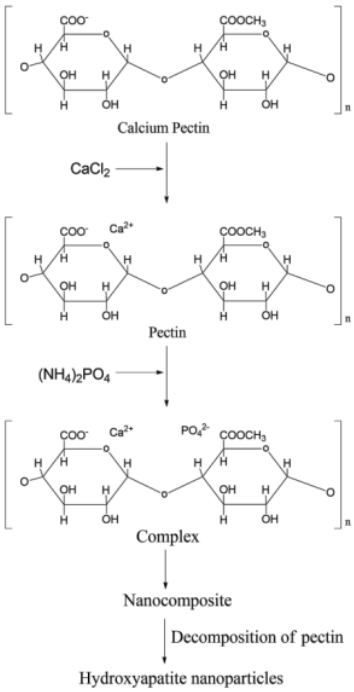

Figure 3. Formation mechanism of HAp nanoparticles

Table 2. The crystal size and degree of crystallinity of the HAp synthesized from each variation

Sampel	Crytal size (nm)	Crystalllinity(%)
HAp K5%	39.9237	70.3430
HAp K10%	37.5358	74.0644
HAp K15%	34.7379	89.7748

HAp Characterization Using BET

The surface area, pore size, and pore volume of HAp of each variation of synthesis results were analyzed to identify its physical and chemical properties. The analysis was carried out using the Brunauer-Emmett-Teller (BET) method, and the adsorption-desorption plot shown in **Figure 4**. showed that HAp of each variation showed a shape similar to the type IV physisorption isotherm and the type H3 loop. It indicates the formation of secondary pores in larger gaps in the nanoparticle aggregates [19].

The results of the analysis of pore volume and pore diameter of particles in HAp of each variation using the BET method are shown in **Table 3**. In this case, the pore diameter can determine the type of pores in HApparticles, significantly affecting their physical and chemical properties. Of the three HApvariations, the synthesis results have an average pore diameter of 7 nm. Thus, it can be concluded that the HAp of each variation of the synthesis results is included in the mesoporous category [20].

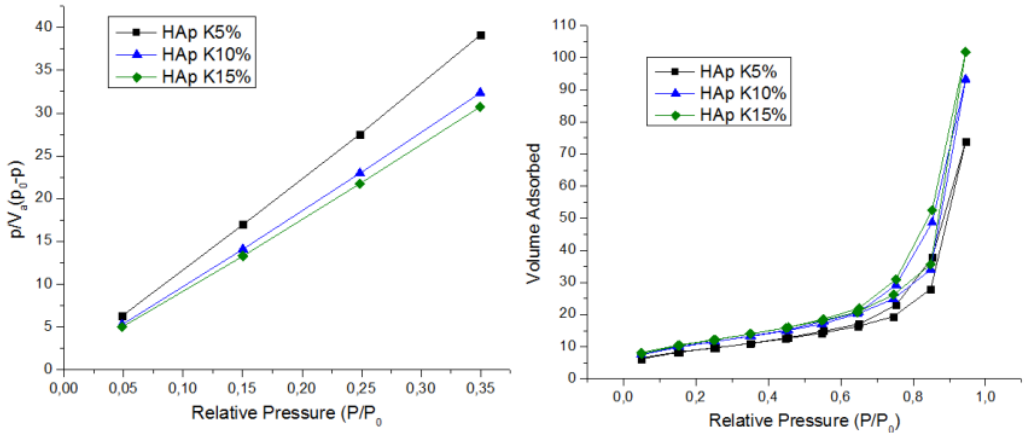

Figure 4. Linear plot of BET equation & adsorption-desorption isotherm HAp for each variation

Table 3. Measurement results with BET HAp for each variation

Sample	Pore Size (nm)	Surface Area (m^2/g)	Pore Volume (cc/g)
HAp K5%	7.2178	30.111	0.1145
HAp K10%	7.5536	39.664	0.1446
HAp K15%	7.8164	42.316	0.1577

The table above shows that of the three HAp variations. HAp, with a 15% green template concentration, has a larger pore volume and diameter than other variations, which are 0.1577 m2/g and 7.8164 nm. It is in accordance with the effect of the green template on the HAp synthesis process and the characteristics produced. In HAp synthesis, the green template can act as a pore former that maintains the initial template structure, thus affecting the pore size and porosity formed. Therefore, the use of green template in hydroxyapatite synthesis can affect the pore size and porosity produced, which is essential in the application of HAp as a drug delivery system [21].

HAp toxicity test on CV-1 cells

Toxicity testing is significant as a parameter for biomedical applications because biocompatibility is one of the critical parameters that need to be considered in the selection of materials in the medical field. Biocompatibility is defined as the ability of a material to provide an excellent biological response when applied to the body [22].

Toxicity testing is carried out in vitro using cell cultures to detect the presence of antineoplastic activity from a compound. The results of the HAp K15% toxicity test on CV-1 cells are shown in **Table 4**, with variations in HAp concentrations of 7.81, 15.63, 31.25, 62.50, 125.00, 250.00, and 500.00

μg/mL in each cell. Dilution is carried out to allow for a more accurate measurement of cytotoxic activity. By changing the sample concentration, the critical point at which these substances begin to show toxic effects can be determined [23].

Table 4. Percentage of live cells HAp K15% toxicity test

Sample (μg/mL)	Percentage of living cells(%)
Media & sel (+)	101.76
Cisplatin (-)	29.94
29.94	109.62
7.81	105.16
15.63	103.21
31.25	98.30
62.50	94.93
125.00	86.96
250.00	67.16
500.00	109.62

The analysis results showed the highest percentage of living cells at a concentration of 7.81 μg/mL with a percentage of living cells of 109.62%. The high percentage of living cells is due to the optical density value of the sample, which is getting closer to the optical density value of the control. Based on ISO 10993-5:2009 (Part E), the results of the toxicity test on cells show that HAp at each concentration is not toxic because the growth of living cells exceeds the toxic limit of 50% (grade 2) and can potentially be used as a drug delivery system. However, the table above shows that the higher the concentration of HAp, the smaller the percentage of living cells. Therefore, in its application, it must be noted that high concentrations of HAp can increase its toxic properties. It can be seen in the cell morphology, indicating that the higher the concentration of HAp, the greater the damage to the morphology. The morphology can be seen in **Figure 5**.

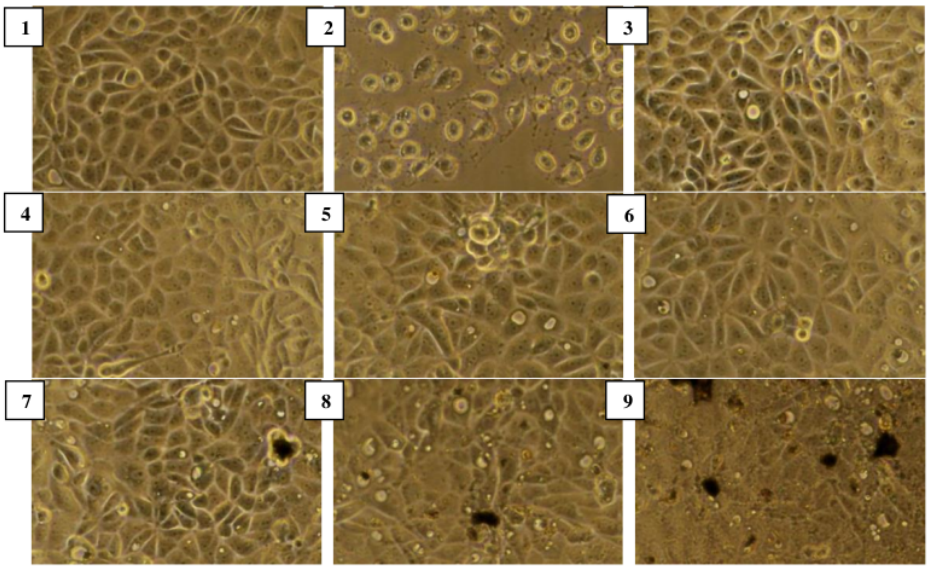

Figure 5. Control (+); 2) Control (-); 3) 7.81 4) 15.63; 5) 31.25; 6) 62.50; 7) 125.00; 8) 250.00; 9) 500.00

Drug loading and drug release

The drug loading test was carried out for 24 hours to determine the efficiency of drug loading into HAp. The drug release test determined the concentration of ibuprofen released in a medium at 30, 60, 90, 120, 150 and 180 minutes at a temperature of 37 °C.

The loading efficiency of ibuprofen HAp K15% of 67.86% is shown in **Figure 6**. In previous research by Singh et al. in 2020, loading ibuprofen drugs on pure HAp only obtained an efficiency value of 33% [24]. It is appropriate because of the pore size, pore volume, and surface area of Hap K15% in the BET results above. Larger pore size, pore volume, and surface area can increase drug loading capacity. The larger the pore size can increase the surface area; likewise, if the available pore volume is larger, the more active substances can be adsorbed or absorbed [25].

The percentage of ibuprofen released in the solution was carried out for 180 minutes with a 30-minute interval, as shown in **Figure 7**. At 60 minutes, there was a spike in its levels; this spike was caused by drug molecules that attached to the surface area quickly, and then there was a slow, linear, and continuous release of the drug when the SBF solvent entered the drug carrier matrix through the pores and diffused [26]. At a later time, there was no spike in the levels of ibuprofen released. However, the release that

occurred to ibuprofen tended to be unstable; this could be associated with uneven drug absorption, where some drugs diffused into the pores of the HAp matrix while the rest attached to the surface [27].

At 60 minutes, there was a significa spike in ibuprofen concentration. This spike can be attributed to drug molecules' rapid attachment to the HAp matrix's surface area. Meanwhile, a study conducted by Singh in 2020 found that pure-HAp nanoparticles showed drug release without a burst release effect, with 30% drug release in the first 25 hours. Although in the first 10 hours, the decline tended to be unstable, like HAp K15% [24].

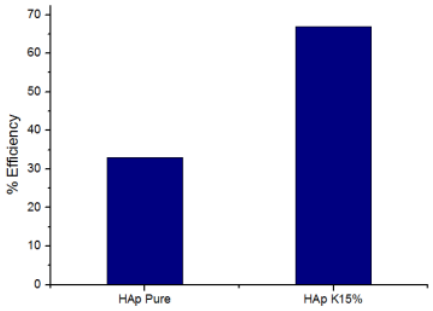

Figure 6. Comparison of pure UAp efficiency with HAp K15%

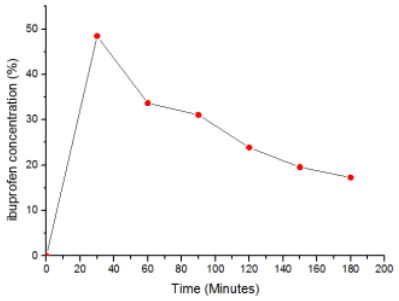

Figure 7. Percentage of ibuprofen released over time interval

This behavior is consistent with the principle of drug release kinetics, where an initial rapid release often occurs due to the presence of drug molecules available on the surface of the carrier material. This phenomenon is commonly observed in drug delivery systems, where surface-bound drugs are released rapidly before a more gradual release of drug molecules embedded in the matrix begins [28]. After this initial spike, the release profile shifts to a slow, linear, and sustained release phase. This sustained release can be explained by the diffusion of artificial body fluid (SBF) solvents into the drug carrier matrix. As the solvent penetrates the pores of the HAp, it facilitates the diffusion of ibuprofen molecules from within the matrix to the surrounding solution. This mechanism is consistent with established drug release theory, where the release rate is influenced by the ability of the solvent to penetrate the matrix and the drug concentration gradient. However, the paper also notes that the subsequent release of ibuprofen did not show a further spike and was characterized by instability. This instability may be related to the uneven adsorption of the drug within the HAp matrix. Specifically, it suggests that while some ibuprofen molecules successfully diffuse into the pores of the HAp, others remain attached to the surface. This uneven distribution may lead to fluctuations in the released ibuprofen concentration over time, as surface-bound drug molecules may be released at different rates than those encapsulated in the matrix [29]. The release behavior of ibuprofen from the HAp matrix reflects a complex interplay between surface attachment, matrix diffusion, and the characteristics of the drug carrier itself. These findings have explored the mechanism of drug release in similar biomaterials, highlighting the importance of understanding the physical properties of the drug carrier and the interactions between the drug and the matrix in optimizing drug delivery systems [30].

4. CONCLUSIONS

Based on the findings of this study, it can be inferred that an increase in the concentration of the green banana peel template significantly influences the properties of the synthesized hydroxyapatite (HAp). The X-ray diffraction (XRD) analysis indicates that using the banana peel template contributes to a reduction in crystal size and an enhancement in crystallinity. Specifically, the crystal sizes observed during HAp synthesis were 39.9237 nm at a 5% concentration, 37.5358 nm at 10%, and 34.7379 nm at 15%. The degree of crystallinity measured varied between 70% and 89%. Additionally, the Brunauer-Emmett-Teller (BET) analysis revealed that the pore sizes across the different concentrations ranged from 7.2 to 7.8 nm, with surface areas between 30 and 42 m^2/g, and pore volumes from 0.11 to 0.15 cc/g. Notably, the HAp synthesized with a 15% concentration of the banana peel template shows promise for application as a drug delivery system. Toxicity assessments on normal cells indicated that viable cells remained above 50%. Furthermore, drug loading experiments conducted over 24 hours achieved a loading efficiency of 67%. However, the results from the drug release studies indicated that the concentration of ibuprofen released at various time intervals (30, 60, 90, 120, 150, and 180 minutes) exhibited instability.

REFERENCES

1. Pepla, Besherat, Palaia, Tenore. Nano-hydroxyapatite and its applications in

preventive, restorative and regenerative dentistry. *Ann Stomatol (Roma)*. 2014;5(2).

2. Basu G, Tripathi B. A porous hydroxyapatite scaffold for bone tissue engineering: Physico-mechanical and biological evaluations. *Ceramics International*. 2012;38(1):341-349.
3. Munir M, Salman S, Javed I. Nano-hydroxyapatite as a delivery system: overview and advancements. *Artificial Cells, Nanomedicine, and Biotechnology*. 2021;49(1):717-727.
4. Ahmed S, Kamil S, Hasso A. Calcium carbonate nanoparticles of quail's egg shells: Synthesis and characterizations. *Journal of the Mechanical Behavior of Materials*. 2022;31:1-7.
5. Yuwanta T. *Telur dan Kualitas Telur*. Yogyakarta: Gadjah Mada University Press; 2010.
6. Yanti, Gandi. Pengaruh Waktu Kalsinasi terhadap Sifat Fisika-Kimia Hidroksiapatit dari Cangkang Gelonia Coaxans. *Chem. Prog*. 2020:102.
7. Suci IA, Ngapa YD. Sintesis dan Karakterisasi Hidroksiapatit (HAp) dari Cangkang Kerang Ale-ale Menggunakan Metode Presipitasi Double Stirring. *Cakra Kimia*. 2020;8(2).
8. Ajeng RA. Penentuan Aktivitas Antioksidan dan Kadar Fenol Total pada Ekstrak Kulit Buah Pisang (Musa acuminata Colla). Paper presented at: Prosiding Seminar Nasional Current Challenges in Drug Use and Development Tantangan Terkini Perkembangan Obat dan Aplikasi Klinis, 2019.
9. Tuhuloula A, Budiyarti L, Fitriana N. Karakterisasi Pektin dengan Memanfaatkan Limbah Kulit Pisang menggunakan Metode Ekstraksi. 2013;2(1):21-27.
10. Abdulkadir S, Hasan H, Alamsyah A. Skrining Fitokimia dan Uji Aktivitas Antioksidan Jantung Pisang Goroho dengan Metode 1,1-diphenyl2- picrylhidrazyl (DPPH). *Indonesian Journal of Pharmaceutical Education*. 2021;1(3):136-141.
11. Noviardi H, Masaenah E, Indraswari K. Antioxidant and Sun Protection Factor Potency of Ambon Banana White (Musa acuminata AAA) Peel Extract. *Jurnal Ilmiah Farmako Bahari*. 2020;11(2):180-188.
12. Schmidta M, Prestesa R, Kubotaa E. Evaluation of antioxidant activity of extracts of banana inflorescences. *CyTA - Journal of Food*. 2015:1-10.
13. Suryanto E, Momuat L, Wehantouw F, Patty W. Potensi Antioksidan Fenolik Dari Famili Myrtaceae Dan Perannya Sebagai Bahan Aktif Tabir Surya. *Chemistry Program*. 2010;3(2):74-80.
14. Aradhya K, Saravanan. Polyphenols of pseudostem of different banana cultivars and their antioxidant activities. *Journal of Agricultural and Food Chemistry*. 2011;59:3613-3623.
15. Ikhlasul Amal A. Sintesis dan karakterisasi hidroksiapatit dari cangkang telur ayam menggunakan Green Template dari tumbuhan pisang (Musa Acuminata Cavendish). *UIN Sunan Gunung Djati Bandung*. 2023.
16. Ramesh S, Tan C, Ting C, Chuah Y, Sutharsini U, dkk. Sintesis dan Sifat-sifat Hidroksiapatit Berbasis Limbah Hayati melalui Proses Hidrotermal. *Materwiss. Werksttech.*. 2020; 51:706-712.
17. Himawan A, Yusuf AJ, Wijaya D, Arjuna A, Arif A, Hasanah N. Evaluasi Efek Inkorporasi Kombinasi Dopan Mg2+ DAN Fe3+ Terhadap Karakteristik Optik dan Struktur Nanoplatform Teranostik ZnO. *Majalah Farmasi dan Farmakologi*. 2020;23(3):112-117.
18. Begum Y, Deka S. Sintesis Hijau Nanopartikel Hidroksiapatit Termediasi Pektin dari Bonggol Pisang Kuliner dan Karakterisasinya. *Acta Aliment*. 2017;46:428-438.
19. Noviyanti R, Akbar N, Deawati Y, et al. A novel hydrothermal synthesis of nanohydroxyapatite from eggshell-calcium-oxide precursors. *Heliyon*. 2020;6.
20. Gultom P, Samuel R. Sintesis dan karakterisasi serbuk hidroksiapatit skala sub-mikron menggunakan metode presipitasi. *Jurnal Bionatura*. 2008;10(2):155-1671.
21. Susanto R, Yuza B, Hermawan DA, Fadli A. Potensi Pembuatan Replika Tulang Berpori Menggunakan Template Ampas Tebu. *Chempublish Journal*. 2020;5:116-129.
22. Anusavice. *Phillips' Science Of Dental Materials*. Pennysylvania: Saunders Company; 2012.
23. Ayu Diah P, Any J, Dewi W. *Uji Toksisitas Akut Limbah Cair Kampung Batik Giriloyo Terhadap Ikan Mas (Cyprinus carpio) Dengan Menggunakan Reaktor Kombinasi Anaerob-Aerob*. Yogyakarta: Universitas Islam Indonesia; 2018.
24. Singh G, Singh S, Singh RP, Pal. Cerium substituted hydroxyapatite mesoporous nanorods: Synthesis and characterization for

drug delivery applications. *Materials Today: Proceedings*. 2020;28(3):1460-1466.

25. Hartono S, Budi H, Lannie A. Pembuatan, Modifikasi dan Pemanfaatan Material Nano-Pori. *Jurnal ilmiah widya teknik*. 2017;16(2):106-108.
26. Pal R, Pal J, Pal A, Kaur A. Encapsulation of vancomycin in copper doped hydroxyapatite mesoporous nanoparticles of different morphologies. *Sci. Technol J Drug Delivery*. 2020;55:101-441.
27. Agustin R, Zaini E, Sari N. Pelepasan Ibuprofen dari Gel Karbomer 940 Kokristal Ibuprofen-Nikotinamida. *Jurnal Sains Farmasi & Klinis*. 2014;1(1):79-88.
28. Subrata K, Banani K, Ruma S, Papiya N, Ruma B, Sukhen D. Curcumin ameliorates the targeted delivery of methotrexate intercalated montmorillonite clay to cancer cells. *European Journal of Pharmaceutical Sciences*. 2019;135:91-102.
29. G B, K R, Fawzi B, Shoaib A, SungMun L, Nouf BS. Mesoporous hydroxyapatite nanoplate arrays as pH-sensitive drug carrier for cancer therapy. *Materials Research Express*. 2019;6.
30. Singh P, Singh P, Amandeep P, Tejinder K. Encapsulation of vancomycin in copper doped hydroxyapatite mesoporous nanoparticles of different morphologies. *Journal of Drug Delivery Science and Technology*. 2020;55.
31. Lugo R, Rodriguez S, Vazquez R. Hydroxyapatite synthesis from a starfish and β-tricalcium phosphate using a hydrothermal method. *Royal Society of Chemistry*. 2017;7:7631.

paper kimia valensi

ORIGINALITY REPORT

14%	8%	10%	2%
SIMILARITY INDEX	INTERNET SOURCES	PUBLICATIONS	STUDENT PAPERS

PRIMARY SOURCES

1	M Sirait, K Sinulingga, N Siregar, M E Doloksaribu, Amelia. "Characterization of hydroxyapatite by cytotoxicity test and bending test", Journal of Physics: Conference Series, 2022 Publication	1%
2	perpustakaan.poltekkes-malang.ac.id Internet Source	1%
3	Gurdyal Singh, Sukhwinder Singh Jolly, Ravinder Pal Singh. "Cerium substituted hydroxyapatite mesoporous nanorods: Synthesis and characterization for drug delivery applications", Materials Today: Proceedings, 2020 Publication	1%
4	Restina Bemis, Ratih Dyah Puspitasari, Heriyanti Heriyanti, Rahmi Rahmi, Gessy Tri Priyanti. "The Effect of Variations of Hydrothermal Temperatures on Ex-Situ Hydroxyapatite/Al2O3 Doping Process from	1%

Papai Shrimp (Acetes erythraeus)", al-Kimiya, 2023
Publication

5	Azhari Yusuf, Norman Maulana Muhammad, Atiek Rostika Noviyanti, Risdiana. "The Effect of Temperature Synthesis on the Purity and Crystallinity of Hydroxyapatite", Key Engineering Materials, 2020 Publication	1 %
6	Gopi, D., K. Kanimozhi, N. Bhuvaneshwari, J. Indira, and L. Kavitha. "Novel banana peel pectin mediated green route for the synthesis of hydroxyapatite nanoparticles and their spectral characterization", Spectrochimica Acta Part A Molecular and Biomolecular Spectroscopy, 2014. Publication	1 %
7	Submitted to ssu Student Paper	1 %
8	www.mdpi.com Internet Source	1 %
9	Awan Maghfirah, Rahelda Irene Sidauruk. "Utilization Of Kijing (Pilsbryoconcha exilis) Shell Waste As A Source Of Hydroxyapatite By Double Stirring And Precipitation Methods As Biomaterials", Journal of Physics: Conference Series, 2024 Publication	1 %

10	Atiek Rostika Noviyanti, Nur Akbar, Yusi Deawati, Engela Evy Ernawati, Yoga Trianzar Malik, Retna Putri Fauzia, Risdiana. "A novel hydrothermal synthesis of nanohydroxyapatite from eggshell-calcium-oxide precursors", Heliyon, 2020 Publication	1 %
11	www.intechopen.com Internet Source	1 %
12	coek.info Internet Source	<1 %
13	M. R. Mohammadi, M. C. Cordero-Cabrera, M. Ghorbani, D. J. Fray. "Synthesis of high surface area nanocrystalline anatase-TiO2 powders derived from particulate sol-gel route by tailoring processing parameters", Journal of Sol-Gel Science and Technology, 2006 Publication	<1 %
14	Silvia Reni Yenti, Ahmad Fadli, Wisrayetti, Amun Amri et al. "Synthesis of hydroxyapatite powder using natural latex particles as pore-creating agent", Materials Today: Proceedings, 2023 Publication	<1 %
15	Shan, Z.. "Mesoporous tungsten titanate as matrix for matrix-assisted laser	<1 %

desorption/ionization time-of-flight mass spectrometry analysis of biomolecules", Analytica Chimica Acta, 20070612
Publication

16	jurnal.untan.ac.id Internet Source	<1 %
17	Tseng, S.H.. "Prevention of hepatic oxidative injury by Xiao-Chen-Chi-Tang in mice", Journal of Ethnopharmacology, 20070504 Publication	<1 %
18	jsfk.ffarmasi.unand.ac.id Internet Source	<1 %
19	pubs.acs.org Internet Source	<1 %
20	acikerisim.sakarya.edu.tr Internet Source	<1 %
21	journals.plos.org Internet Source	<1 %
22	vc.bridgew.edu Internet Source	<1 %
23	Isaac Rodríguez-Ruiz, José Manuel Delgado-López, Miguel A. Durán-Olivencia, Michele Iafisco et al. "pH-Responsive Delivery of Doxorubicin from Citrate–Apatite Nanocrystals with Tailored Carbonate Content", Langmuir, 2013	<1 %

Publication

24	K Fibrianto, B S Muliadi, C A Tedja, A Hartari, A M Legowo, A N Al-Baarri. " Brewing characterization for optimum functional properties of Dampit Robusta ( ) and Liberica ( ) coffee leaves tea ", IOP Conference Series: Earth and Environmental Science, 2020 Publication	<1 %
25	Margarita A. Goldberg, Nadezhda O. Donskaya, Dmitry V. Valeev, Alexander S. Fomin et al. "Mesoporous molybdate-substituted hydroxyapatite nanopowders obtained via a hydrothermal route", Ceramics International, 2024 Publication	<1 %
26	Nanti - Musita. "Characteristics of Pectin Extracted from Cocoa Pod Husks", Pelita Perkebunan (a Coffee and Cocoa Research Journal), 2021 Publication	<1 %
27	www2.mdpi.com Internet Source	<1 %
28	Ebru Kahraman, Gulhayat Nasun-Saygili. "5-Fluorouracil adsorption on graphene oxide-amine modified graphene oxide/hydroxyapatite composite for drug delivery applications: Optimization and release kinetics studies", Heliyon, 2024	<1 %

	Publication	
29	Michele M. Schmidt, Rosa C. Prestes, Ernesto H. Kubota, Gabrielle Scapin, Marcio A. Mazutti. " Evaluation of antioxidant activity of extracts of banana inflorescences ( ) ", CyTA - Journal of Food, 2015 Publication	<1 %
30	link.springer.com Internet Source	<1 %
31	mts.intechopen.com Internet Source	<1 %
32	www.grafiati.com Internet Source	<1 %
33	www.jwent.net Internet Source	<1 %
34	www.researchgate.net Internet Source	<1 %
35	www.scientific.net Internet Source	<1 %
36	He, N.Y.. "Catalytic formation of acetic anhydride over tungstophosphoric acid modified SBA-15 mesoporous materials", Applied Catalysis A, General, 20050318 Publication	<1 %

Exclude quotes	On	Exclude matches	Off
Exclude bibliography	On		